

1 Estimating individual growth variability in albacore (*Thunnus alalunga*) from the North Atlantic  
2 stock; aging for assessment purposes.

3

4

5 V. Ortiz de Zárate <sup>1</sup> & E. A. Babcock <sup>2</sup>

6

7 <sup>1</sup> Instituto Español de Oceanografía, P.O. 240, 39080 Santander, Spain.

8 (e-mail: victoria.zarate@st.ieo.es)

9 <sup>2</sup> Rosenstiel School of Marine & Atmospheric Science, University of Miami, 4600 Rickenbacker  
10 Causeway, Miami, Florida 33149, USA. (e-mail: ebabcock@rsmas.miami.edu)

11 *Keywords*

12 *Thunnus alalunga*, albacore, back-calculation, Bayesian modelling, growth curves

13

14 **ABSTRACT**

15 Length-frequency data and derived catch at age matrices are used in north Atlantic albacore  
16 (*Thunnus alalunga*) stock assessment conducted within the International Commission for the  
17 Conservation of Atlantic Tunas (ICCAT). Growth is assumed to follow the von Bertalanffy  
18 model with the assumption that growth parameters are constant over time and the same for all  
19 fish. However individual growth variability is an important factor not considered and affecting  
20 the input into the modelling of the population. This study describes a Bayesian hierarchical  
21 model applied to model the individual variability in the parameters asymptotic length ( $L_{\infty}$ ) and  
22 growth rate ( $K$ ) of the von Bertalanffy growth model for North Atlantic albacore. The method  
23 assumes that the  $L_{\infty}$  and  $K$  values for each individual fish are drawn from a random distribution  
24 centered on the population mean values, with estimated variances. Multiple observations of spine  
25 diameter at age for individual fish were obtained by direct reading of spine sections collected in  
26 2011 and 2012. A suite of back calculation methods were then applied to the measurements of  
27 annuli diameters in the aged individuals observed to back-calculate lengths at each age. The von  
28 Bertalanffy model was fitted to the measured and back-calculated lengths. Models with and  
29 without individual growth variability were compared using the deviance information criterion  
30 (DIC) to find the best model. Normal and log-normal error distribution models were used to  
31 analyse the data. Additionally, subsamples of the data were used to evaluate whether an  
32 unbalanced age-distribution in the data affects estimates of growth parameters. It was found that  
33 North Atlantic albacore asymptotic length ( $L_{\infty}$ ) varies significantly between individual fish but  
34 not individual rate growth ( $K$ ), for all back-calculation methods. Furthermore, negatively  
35 correlated relationships between von Bertalanffy growth parameters of asymptotic mean ( $L_{\infty}$ )  
36 and growth rate ( $K$ ) were estimated for North Atlantic albacore with the array of models

37 explored. The overall estimated values of  $K$  and population mean  $L_{\infty}$  parameters were similar to  
38 values estimates in previous north Atlantic albacore growth studies.

39

## 40 **Introduction**

41

42 Atlantic albacore tuna (*Thunnus alalunga*) is large pelagic fish that inhabits the temperate and  
43 subtropical waters of the Atlantic Ocean. It is an economically important species that is managed  
44 under the International Commission for the Conservation of the Atlantic tunas (ICCAT). In the  
45 Atlantic three stocks are identified for assessment purposes: North and South Atlantic separated  
46 at 5° N in the Atlantic and a third Mediterranean stock (ICCAT, 2006-2013). Commercial  
47 fisheries in the Northern Atlantic have targeted the albacore stock by surface fisheries since the  
48 1930s and longline fleets beginning in the 1950s (ICCAT, 2013a). The surface fishery represents  
49 roughly 80% of the total catch and the longliners account for 20 % in the last two decades  
50 (ICCAT, 2014). The surface fishery includes three different type of vessels according to the  
51 gears: mid-water pair pelagic trawls, trollers and baitboats. Spanish baitboats and troll landings  
52 represent an approximate participation in the fishery between 55 to 65% of the total annual  
53 surface fishery landings from the North Atlantic stock.

54

55 The last assessment of North Atlantic albacore stock, performed in 2013, reported substantial  
56 uncertainty on the current stock status considering the set of models applied, but it was concluded  
57 that the status of the spawning stock biomass was overfished (ICCAT, 2014).

58

59 North Atlantic albacore are assessed with a variety of models, including a length based model  
60 (Multifan-CL) that requires a growth curve as input, and two other models: VPA and Stock  
61 Synthesis (SS) that are fitted to catch-at-age data calculated from catch-at-length data using a  
62 von Bertalanffy (von Bertalanffy, 1938) growth curve (ICCAT, 2013a). Moreover, the growth  
63 function is used to derive reference points for sustainable management (Beverton and Holt, 1957;  
64 ICCAT, 2013a).

65

66 Direct aging data have been used to study growth. A number of studies have been conducted  
67 to describe the growth of northern albacore (Bard and Compeán-Jimenez, 1980; Bard, 1981;  
68 Gonzalez-Garcés and Fariña-Perez, 1983) based on reading of the first fin ray of the first dorsal  
69 fin to determine age and fit a von Bertalanffy (von Bertalanffy, 1938) growth model, considering  
70 constant parameters for the population. The most recent study, assumed constant parameters and  
71 used the first dorsal fin ray section readings along with updated release and recapture tag data in  
72 an integrated model to fit the von Bertalanffy function (Santiago and Arrizabalaga, 2005). The  
73 analysis of the North Atlantic albacore population (ICCAT, 2014) has incorporated knowledge  
74 on the growth biology based on Bard's (1981) growth model and Santiago and Arrizabalaga's  
75 (2005) growth estimates to characterize the population dynamics of the north Atlantic albacore  
76 stock. The catch- at-size data for northern stock is analyzed to derive an annual age-length key  
77 (ALK) by applying the Kimura and Chikuni iterative method (1987) and using Bard's (1981)  
78 growth parameters (ICCAT, 2014; Ortiz, 2014).

79

80 Generally, when growth models are fitted to length-at-age data, only one observation is available  
81 for each individual animal. Therefore, it is not possible to determine what fraction of the variation  
82 in measured length is due to measurement error, and what fraction is due to variation in growth  
83 between individual fish. Thus, the residual error in a fitted growth model includes both individual  
84 variation and measurement error. When multiple observations are available for each individual,  
85 for example from tag-and-recapture data, it is possible to evaluate how much individual variation  
86 exists in the growth model parameters, and to estimate the correlation between growth parameters  
87 across individual fish (Zhang *et al.* 2009).

88

89 None of the growth models use in the assessment of the North stock albacore incorporate  
90 individual variability in the von Bertalanffy growth function parameters. However individual  
91 variation in growth is expected depending on physiological and environmental conditions. The  
92 first model incorporating individual variation in the  $K$  and  $L_{\infty}$  von Bertalanffy growth parameters  
93 was described by Sainsbury (1980); later Kirkwood and Sommers (1984) continued investigating  
94 variation in maximum length between individuals. Moreover, Hampton (1991) modified those  
95 approaches incorporating a model error component and estimates of a release length  
96 measurement error term fitted by maximum likelihood. The available North Atlantic albacore  
97 tag-release data were analysed to estimate von Bertalanffy growth parameters based on  
98 Hampton's model that incorporates individual variation in growth, release length measurement  
99 error and model error terms (Ortiz de Zárate and Restrepo, 2001).

100

101 Back calculation methods are employed to estimate length of a fish at previous age based on  
102 reading of calcified structures such as: otoliths, scales and fin rays (spines), among other skeleton  
103 structures. This technique re-creates the life history of individual fish. This method assumes that  
104 there is a relationship between the length of the fish and the skeleton structure, either linear or  
105 allometric (Bagenal, 1978; Campana, 1990; Francis, 1990; Folkvord and Mosegaard, 2002;  
106 Ricker, 1992).

107

108 One albacore spine aging study used a linear relationship recommended by Campana (1990) to  
109 back-calculate lengths (Santiago and Arrizabalaga, 2005); meanwhile other spine studies  
110 incorporated proportional methods to back-calculate lengths (Cheng *et al.*, 2012; Duarte-Neto *et al.*,  
111 2012; Kopf *et al.*, 2011; Sardenne *et al.*, 2014). Methods for back-calculation of length-at-age  
112 generally assume that the relationship between fish length and hard part diameter is a family of  
113 lines radiating from a common point near the origin, with different slopes for each fish (Francis,  
114 1995). This assumption allows individual fish lengths to vary more when they are larger than  
115 when they are smaller, which is biologically reasonable and performs well in simulation studies  
116 (Schirripa, 2002). However, which back calculation method is best suited to be applied may  
117 depend on the functional form of relationship between length and annulus diameter, and other  
118 growth characteristics that may vary between stocks (Schirripa, 2002). In the thorough review of  
119 types of back-calculation methods by Francis (1990), he recommended that both regression of  
120 body length-scale to scale radius (BPH) and scale radius- to body length (SPH) be used for each  
121 fish population because neither is clearly preferable. Later, Ricker (1992) proposed the geometric  
122 mean regression using both relationships named by Francis (1990) to estimate the y-intercept for  
123 the back-calculation of length from hard structures annuli, in the absence of any biological  
124 intercept estimate. This method was applied by Pilling *et al.* (2002) to back-calculate lengths

125 from otolith radius counts over the life span of a number of individuals of tropical emperor  
126 (*Lethrinus mahsena*) and the lengths were used to fit models that incorporated individual  
127 variation in growth.

128

129 The objective of this paper is to use multiple length and age reading estimates for individual  
130 albacore tuna, where lengths were back-calculated from the measured diameters of the annuli  
131 readings of cross-sections of first dorsal fin ray (spine), to evaluate how much the growth  
132 parameters vary between individual fish in the North Atlantic albacore population. Growth  
133 models were fitted and evaluated using Bayesian hierarchical models. Several alternative back-  
134 calculation models were used to determine whether the choice of back-calculation method  
135 influences the estimated growth curve parameters or the conclusions about individual variation.  
136 Finally, alternative sub-sets of the data were used to evaluate whether differences in sample sizes  
137 across ages influenced the results, and whether using back-calculated lengths gave different  
138 average results from using lengths at capture only. This study is the first attempt to use an array  
139 of back-calculated lengths from spine measured annulus to estimate growth parameters for North  
140 Atlantic albacore incorporating individual variability in the von Bertalanffy function model.

141

142

## 143 **Material and Methods**

144

### 145 *Sampling of spines (first fin ray)*

146

147 As part of the monitoring of the activity of the Spanish albacore (*Thunnus alalunga*) fisheries,  
148 biological samples are collected from the landings at the main fishing ports (Ortiz de Zárate *et al.*  
149 2013; Ortiz de Zárate *et al.* 2015, *in press*). A number of trips were sampled to obtain the length  
150 frequency of the catch by applying random sampling stratified according to commercial  
151 categories of catches landed at the main fishing markets. Random samples of the first fin ray  
152 (spine) from the first dorsal fin were removed during the albacore length sampling procedure. For  
153 each fish, the total fork length (FL) to the nearest centimeter, date, and catch area were noted.  
154 Spines were collected based on a length-stratified sampling protocol by 1 cm class length,  
155 covering the whole length range of albacore landings. Sampling design of spines was stratified by  
156 spatial and temporal strata. Collection of spines was done once a week at selected fishing ports,  
157 covering different geographical areas (1°x1° degrees), during the fishing season, from June to  
158 November in the Northeast Atlantic (Figure 1). The samples in this study were collected during  
159 the 2011 and 2012 albacore fishing seasons and no sex information was recorded. The length  
160 composition of all albacore sampled is displayed in Figure 2.

161

### 162 *Ageing from spine readings*

163

164 The criteria used to interpret the pattern of observed translucent or hyaline bands (annuli) formed  
165 on the spine cross sections of albacore, was based on the hypothesis of Bard and Compeán  
166 (1980), which assumes that the formation of two annuli per year throughout the life span of North  
167 Atlantic albacore corresponding to its migratory behaviour between feeding (spring-summer/

168 autumn-winter) and spawning grounds (Bard, 1981). Albacore birth date was assumed to be the  
169 first of June, in agreement with a protracted spawning period from March to October, with a peak  
170 in June-July (ICCAT, 2006-2013) in the North Atlantic Ocean. For age determination, the first  
171 visible annulus was identified as formed during the first migration of juvenile albacore from the  
172 spawning area to the wintering area at an approximate age of six months (Bard, 1981). The  
173 appearance of the first annuli has been validated with daily increments reading on otoliths from  
174 the North Atlantic albacore (Lu *et al.*, 2007) and daily increments readings on otoliths of Pacific  
175 albacore (Bigelow *et al.*, 1993, 1995). Then the successive annual mark formed by double annuli  
176 (spring-summer and autumn) and a dark growth band was assigned to age group 1 and, by  
177 counting successive annual marks formed, the age of each fish was determined. If an autumn  
178 annulus was already formed, age was determined as belonging to the same year class (i.e. 1 year  
179 class). Some spine sections had formed a single translucent annulus and dark growth zone, as an  
180 annual mark, however, in the majority of spines the double spring-summer annuli and dark  
181 growth zone annual pattern was visible. For north Atlantic albacore, oxytetracycline injections of  
182 tagged albacore released and recaptured, being at liberty one and two years, although samples  
183 size was small (n=21), seemed to verify that one annulus is formed on spring-summer and  
184 another in autumn, likewise, an alternative observed pattern in adult albacore (> 5 years), was  
185 defined by forming one annulus per year, consequently a single annulus and dark zone was  
186 associated with a given age in some older individuals (Ortiz de Zárate *et al.*, 1996). Recently a  
187 north Atlantic albacore growth study using spine readings, suggested that one of the annual rings  
188 is formed mainly between July and September (Santiago and Arrizabalaga, 2005). Occasionally,  
189 vascularization obscured the first double annuli, the spring one for age 1 and occasionally even  
190 for age 2, or either spring or autumn annuli or both, in older fish. Estimated mean annulus  
191 diameter (mm) and standard deviation (s.d.) for age group 1, 2 and 3 by month were applied to  
192 identify the corresponding first visible annulus and the following visible annuli were counted  
193 from this value (Ortiz de Zárate *et al.*, 2005). In our study, the identified first annuli represented  
194 16% (autumn annulus age 1) and 2.6% (spring-summer or autumn annulus age 2) of the two  
195 combined year sample.

196 The aging method used in our study was tested previously to estimate the precision and relative  
197 bias by applying the procedure described by Eltink (2000) among three readers. The overall  
198 coefficient of variation (CV) was 8.5% and an overall agreement of 82% between readers was  
199 observed (Ortiz de Zárate *et al.* 2005), which implied a good level of precision (Campana, 2001;  
200 Campana *et al.*, 1995). For this study, only one reader was generally involved in readings. In  
201 2011, a sub-sample of 75 fish and in 2012, a subsample of 175 fish, including many of the older  
202 fish where ages might be more ambiguous, were read by two readers independently. Age  
203 readings were compared with two different tests of symmetry using  $\chi^2$  statistics (Bowker, 1948;  
204 Evans and Hoenig, 1998). Precision between readers was estimated with a new approach  
205 developed by McBride (2015) and implemented on template by S. Sutherland (NOAA). The  
206 results of the two independent readers showed no evidence of asymmetry in 2011, for the  
207 Bowker's test of symmetry (Chi.sq= 13.33; d.f.=10,  $p= 0.21$ ) and Evans and Hoenig's test  
208 (Chi.sq= 1.84; d.f.=3,  $p= 0.61$ ). In 2011, the estimated CV was 9.7 %, considered an acceptable  
209 value (Campana, 2001). Comparison of the two independent readings in 2012 shows evidence of  
210 asymmetry for the Bowker's test (Chi.sq= 18.9; d.f.=8,  $p= 0.015$ ), but for the Evans-Hoenig's test  
211 (Chi.sq= 7.79; d.f.=3,  $p= 0.051$ ) the null hypothesis of symmetry could not be rejected. The

212 estimated CV among two readers was 8.6 %. The number of samples that disagreed were 24 and  
213 50 in 2011 and in 2012 respectively. Those samples were read again jointly by the two readers  
214 and agreement was reached to a final age. Only 2 and 3 spines from the last joint reading were  
215 discarded in the two consecutive years 2011 and 2012. The final sample used for the analysis  
216 included all the single-reader ages, and the agreed ages from the double-reader subsample.

217 Finally, based on the annuli pattern formation having either the spring-summer or the autumn  
218 annulus close to the edge of the section read and the date of capture, only one single annulus  
219 measured diameter, either spring or autumn, in all the annual double annuli read was used in the  
220 back-calculation of length to obtain the growth trajectory of each individual fish.

221

## 222 *Statistical analysis*

223

### 224 *Growth increment analysis*

225

226 Data were available for fish that were captured in both 2011 and 2012. To evaluate whether there  
227 was any annual variation or variation between cohorts in growth increments, we calculated  
228 annual growth increments for each measured spine diameter. The annual increment was the  
229 change in spine diameter from one spine annulus to the next, divided by the difference in age  
230 between the two spine annulus (usually one year, sometimes 0.75 or 1.25 year depending on  
231 when the fish was captured, and whether the spring-summer or autumn annulus was used; see  
232 *growth model* section below for an explanation of how ages were calculated). A linear model was  
233 used to evaluate the effect of age (as a numerical variable) and cohort (as a factor) on the size of  
234 the annual increment. The interaction between age and cohort was included to evaluate whether  
235 there was an effect of year. To ensure an adequate sample size at each age and cohort, only  
236 cohorts from 2009 and later, for fish of age four or less at the time of the increment formation,  
237 were included.

238

### 239 *Length back-calculation*

240

241 The geometric mean regression (GMR) allows estimation of the y-intercept to apply as a  
242 biological correction factor to mitigate Lee's phenomenon (Lee, 1912) when back calculating  
243 length from spines (Ricker, 1992). The observed data in 2011 and 2012 were combined and fitted  
244 to GMR and simple linear regression models following three methods:

245

246 **Method 1.** The geometric mean regression method (Ricker, 1992; Pilling *et al.* 2002) was used to  
247 calculate the following regression using all the measured fish fork lengths and spine section  
248 diameters at capture from the 2011 and 2012 data sets combined:

249

$$250 \quad (1) \quad S_i = a_s + b_s L_i + \varepsilon_{S,i}$$

251

$$252 \quad (2) \quad L_i = a_L + b_L S_i + \varepsilon_{L,i}$$

253

254 Where  $S_i$  is the spine diameter at capture for fish  $i$ ,  $L_i$  is the length at capture for fish  $i$ ,  $a_S$ ,  $b_S$ ,  $a_L$ ,  
 255  $b_L$  are the regression coefficients, and  $\varepsilon_{S,i}$  and  $\varepsilon_{L,i}$  are normally distributed error terms with means  
 256 of zero, and estimated variances. The parameters of the geometric mean regression,  $a$  and  $b$ , were  
 257 calculated as:

258

$$259 \quad (3) \quad b = \sqrt{b_L / b_S}$$

260

261 and

262

$$263 \quad (4) \quad a = \text{mean}(L_i) - b \cdot \text{mean}(S_i)$$

264

265 Then the Fraser-Lee (Fraser, 1916, Lee, 1920) proportional model was applied to back-calculate  
 266 lengths ( $L_{i,j}$ ) for the all the measured annuli for each individual fish using the following equation:

267

$$268 \quad (5) \quad L_{i,j} = \frac{(L_i - a)S_{i,j}}{S_i} + a$$

269

270 Where  $L_i$  is the length of fish  $i$  at capture,  $S_i$  is the spine diameter at capture,  $L_{i,j}$  is the back-  
 271 calculated length age  $j$ ,  $S_{i,j}$  is the spine diameter at age  $j$  and  $a$  is the y-intercept from the GMR  
 272 regression. The standard error  $e_{i,j}$  of  $L_{i,j}$  is assumed to equal the standard error calculated from the  
 273 regression of  $L$  on  $S$ .

274

275 **Method 2.** The geometric mean regression (GMR) on log-transformed data (Ricker 1992,  
 276 Folkvord and Mosegaard, 2002) was fit to the combined data set to estimate the constant of  
 277 allometry ( $v$ ).

278

279

$$280 \quad (6) \quad \log(S_i) = \alpha_S + \beta_S \log(i_i) + \varepsilon_{S,i}$$

281

$$282 \quad (7) \quad \log(L_i) = \alpha_L + \beta_L \log(S_i) + \varepsilon_{L,i}$$

283

$$284 \quad (8) \quad v = \sqrt{\beta_L / \beta_S}$$

285

286 Then the method proposed by Monastyrsky (1930) was used to back-calculate lengths ( $L_{i,j}$ ) for all  
 287 the measured annuli for each individual fish using the following equation:

288

$$289 \quad (9) \quad L_{i,j} = \left( \frac{S_{i,j}}{S_i} \right)^\beta L_i$$

290

291 The standard error  $e_{i,j}$  of  $L_{i,j}$  is assumed to equal the standard error calculated from the regression  
 292 of  $\log(L)$  on  $\log(S)$ , converted from normal to lognormal.

293

294 **Method 3.** When back-calculated lengths are used to fit a growth curve, the choice of back-  
295 calculation model may constrict the amount of individual variation the growth model can  
296 estimate in each of the growth parameters (Francis, R.I.C.C., personal communication, Francis  
297 1995). To test whether the use of a proportional back-calculation method influenced the degree of  
298 individual variation in the growth parameters, a back calculation method was applied that did not  
299 make this assumption. The simple linear regression of log of spine diameter at capture against log  
300 of length at capture (equation 7) was applied. The same equation was used to infer the back  
301 calculated lengths at previous ages from the measured annuli at previous ages. Linear regression  
302 implies that the same slope between  $L$  (length) and  $S$  (diameter spine) can be applied to all fish.  
303 This simplified approach is not recommended for back-calculation because the proportional  
304 methods have been found to be more accurate (Guteuter, 1987; Francis, 1990; Folkvord and  
305 Mosegaard, 2002; Schirripa, 2002). However, the method is useful for testing the hypothesis,  
306 proposed by Francis (1995), that the individual variation found in the growth curve is a  
307 consequence of the assumed back-calculation method.

308

309 All regressions and back-calculations were conducted in R version 3.1.2 (R Core Development  
310 Team 2015). The means and standard errors of the predicted lengths from each back-calculation  
311 method were used as inputs to the growth models (see next section).

312

313 Graphical tools were used to examine for homogeneity and normality of the data being regressed  
314 (Zuur *et al.*, 2010). The predicted mean length at age estimated by the three methods were  
315 examined for comparison across methods and against measured lengths.

316

317 *Growth models*

318

319 A quarterly cycle was determined to describe annual variability in growth with relation to birth  
320 date. Thus for each individual fish, the decimal age at capture was estimated based on the quarter  
321 in which the fish was captured. Fish captured in June were age  $x.0$ , fish captured in July, August  
322 or September were age  $x.25$ , and fish captured October, November or December were age  $x.5$ ,  
323 where  $x$  is the age in years inferred from the spine reading. For every fish, the measured length  
324 and age at capture were used in the model fitting. For fish aged 2 or more, back-calculated ages  
325 and lengths were used for all the ages prior to capture for which an annulus was visible. The  
326 back-calculated lengths were assumed to apply to ages that were either  $x.0$  or  $x.25$  years of age,  
327 depending on whether the spring-summer or the autumn band was measured.

328

329 The multiple observations from 2011 and 2012 of measured and back-calculated lengths and ages  
330 were used to fit the parameters of the von Bertalanffy growth model with possible individual  
331 variation in the growth parameters (Helser and Lai 2004, Zhang et al. 2009):

332

333 (10)  $L_{t,i} = L_{\infty,i} \left( 1 - \exp \left( -K_i (t - t_0) \right) \right) + \varepsilon_{t,i}$

334

335 Where  $L_{t,i}$  is length at age  $t$  for individual fish  $i$ ,  $L_{\infty,i}$  is asymptotic mean length for fish  $i$ ,  $K_i$  is the  
336 growth rate for fish  $i$ , and  $t_0$  is the age at zero length, assumed to be the same for all fish, and  $\varepsilon_i$  is



337 a normally distributed error term with an estimated variance. In the most complex model, both  $K_i$   
 338 and  $L_{\infty,i}$  were estimated as normally distributed random effects with estimated means and  
 339 variances (Table 1). Alternative models treated  $L_{\infty}$ , or  $K$  as constant across the population.

340

341 The variance  $\sigma$  of the error term  $\varepsilon_{t,i}$  was either assumed to be constant across all the data points  
 342 or it was informed by the standard errors of the predicted lengths from the back calculation  
 343 model. For measured lengths, the residual standard deviation was always assumed to be constant.  
 344 For the back calculated lengths, the residual standard deviation was either the same as the  
 345 residual standard deviation of the measured lengths, or it was assumed to be proportional to the  
 346 estimated standard error  $e_{t,i}$  of the length prediction:

347

348  $\sigma_{t,i} = \sigma_{measured}$  if length is measured

349 (11)  $\sigma_{t,i} = e_{t,i} \sigma_{back}$  if length is back-calculated

350 where  $\sigma_{measured}$  and  $\sigma_{back}$  are estimated parameters.

351

352 The majority of the fish in the back-calculated dataset were only one or two years old. Thus, the  
 353 sample size of young fish was much higher than the sample size of older fish. When fitting  
 354 growth curves, a very different sample size in each age category can lead to bias in estimates of  
 355 growth parameters (Thorson and Simpfendorfer, 2009). Therefore, we ran the models with the  
 356 fish subsampled to give a more even sample size among the younger ages. All fish that were  
 357 captured at age 5 or higher were included, but fish captured at age 1 to 4 were sub-sampled so  
 358 that there were roughly 80 fish in each age, including both back-calculated and measured lengths.  
 359 To further evaluate the implications of having an unbalanced sample across ages, we also fit the  
 360 model with only fish age 5 or less.

361

362 As an additional model test, the growth model was fitted to the observed lengths only. With only  
 363 measured lengths, there was only one sample per individual fish, so individual variation in  
 364 growth could not be estimated. To evaluate whether sample size in each age category caused bias  
 365 in the results, the model was fitted to all the observed lengths, and also to a dataset in which the  
 366 younger ages were sub-sampled to a sample size of 30 per age category, and to only fish age 5 or  
 367 under five.

368

369 In addition to the assumed normal error distribution, we fit the growth models with the log-  
 370 normal distribution error and compared the fit of the model.

371

372 (12)  $L_{t,i} = L_{\infty,i} \left( 1 - \exp(-K_i(t - t_0)) \right) e^{\varepsilon_{t,i}}$

373

374

375 The models were fitted in a Bayesian framework, with uninformative priors on all the parameters  
 376 (Table 1). All analyses were conducted in JAGS, which uses the Gibbs sampler form of the  
 377 Markov Chain Monte Carlo (MCMC) algorithm; JAGS was run using the R2Jags package for the  
 378 R statistical software (R Development Core Team 2015, Su and Yajima 2014). Two MCMC

379 chains were run with a burn in of 50,000 and an additional run of 200,000 with a thin of 20. The  
380 Gelman-Rubin diagnostic was used to ensure convergence of the MCMC chains on the  
381 posterior distribution (Gelman, 2007). Models that had not converged according to this diagnostic  
382 were run for an additional 200,000 iterations. To compare models that included individual  
383 variation on different growth parameters, the deviance information criterion (DIC) was used  
384 (Lunn *et al.* 2013). The DIC weights the trade-off between model fit and the number of  
385 parameters estimated, and the model with the lowest DIC is best supported by the data. Only  
386 models fitted to the same back-calculated length data-set can be compared with the DIC.

387

388

389

## 390 **Results**

391

392 In 2011, a sample of 583 spines collected from June to October was examined, for fish ranging  
393 from 41 to 120 cm (FL) size, likewise in 2012, spines examined amounted to 902 in total with a  
394 length range 40 to 112 cm (FL), samples were collected from June to November respectively and  
395 no sex information was available to be incorporated in the analysis.

396

### 397 *Growth increment analysis*

398

399 Of the 1485 individual fish collected in 2011 and 2012, 84% were three years old or younger.  
400 From these fish there were 1891 distinct spine increments (Table 2). The size of the growth  
401 increment declined linearly with the age at which the spine formed, but there was no significant  
402 influence of the cohort on this trend (Table 3). Therefore, for the remainder of the analyses, data  
403 from both years were combined.

404

405

### 406 *Back-calculation models*

407

408 A total number of 1891 annuli observations were used in the three models applied to back-  
409 calculate length.

410

411 The three regression models used for back-calculation of length found high correlation between  
412 the measured length at capture and the diameters of the spine section. Geometric mean regression  
413 (GMR) and simple log-linear regression (Method 1 and Method 3) explained 95% of the variance  
414 on the observed data (adjusted  $R^2 = 0.951$ ,  $p$ -value  $< 0.05$ ,  $a = 15.84$ ,  $b = 14.86$ ), likewise the log-  
415 geometric mean regression (log-GMR) model also showed a high correlation between the length  
416 at capture of fish and the diameter of the spine section, the variance explained was 95% (adjusted  
417  $R^2 = 0.953$ ,  $p$ -value  $< 0.05$ ,  $a = 3.27$ ,  $b = 0.76$  in log scale).

418

419 The dispersion of the residuals against fitted values and the Quantile-quantile (QQ) plots for the  
420 GMR and log-GMR regression model fits are shown in Figures 3a,b,c,d. The residuals indicate  
421 that the regressions on  $\log(L)$  and  $\log(S)$  give the best fit from the point of the distribution of  
422 variance (Figure 3c,d). Therefore the log-GMR model was chosen as the best to back-calculate

423 length and used to fit the different models of growth. Some additional model runs were done  
424 using the GMR for comparison.

425

426 Mean length-at-age back calculated and their standard deviations from each of the three  
427 methods: GMR and Fraser-Lee (1), log-GMR and Monastyrsky (2), log-linear regression (3) and  
428 the observed mean length data are displayed in Table 2. Of the three back-calculation models,  
429 the two GMR methods gave similar mean predicted lengths, particularly for age groups 1 to 5  
430 showing similar variation. For fish above age 5, the observed variation is larger, due to small  
431 sample size for larger fish. The back-calculation approach appears to underestimate the  
432 variability in lengths of younger fish. Overall, the CV of different mean length-at-age did not  
433 exceed 10% neither for the observed nor the three back-calculations methods. The highest CV  
434 was found for the observed mean length of age 1 albacore.

435

436 In the three models, the range of variation in lengths at age was comparable between the mean  
437 predicted lengths and the measured lengths for spines of a similar diameter (Figure 4a, b, c). The  
438 regression did not allow individual fish to have different mean predictions so that its mean  
439 predictions are a simple line (Figure 4d). Method 3 assumes that all variation in length at age  
440 between individual fish is residual error. On the other hand, the proportional back-calculation  
441 methods, are able to predict lengths for particular fish that vary from the mean prediction at a  
442 given spine diameter.

443

444

#### 445 *Growth models*

446

447 When the fish were subsampled to give a roughly similar sample size in the well-sampled ages,  
448 the resulting sample contained 470 observations from 97 individual fish (Figure 5b). Because it  
449 was necessary to keep all the back-calculated lengths for each fish that was selected in the sub-  
450 sample, the younger ages are dominated by back-calculated lengths. Also, it was not possible to  
451 have completely balanced sample sizes in all the younger ages. Nevertheless, the subsample is  
452 more balanced than the complete dataset. The subsample for measured lengths only included 200  
453 fish (Figure 5e).

454

455 For all three back calculation methods, for both the complete sample and a more balanced sub-  
456 sample, we ran models with: (1) individual variation in both  $L_{\infty}$  and  $K$ , (2) individual variation in  
457  $L_{\infty}$  only, and (3) no individual variation. For the log-GMR back-calculation method 2, which we  
458 considered to be the best back-calculation method, models with different error structures were  
459 also considered. With all the combinations of the data sets, error structures, and mixed models ,  
460 there were 27 candidate growth models. All had adequate convergence diagnostics (see  
461 Appendix) and appeared to fit the data well.

462

463 When a balanced sub-sample of the data was used, for all three back-calculation methods the DIC  
464 preferred the growth model that included individual variation in  $L_{\infty}$  but not  $K$  (Table 4). For the  
465 log-GMR and log-regression methods, this model was also preferred when the subsample was  
466 used; however, for the complete dataset using the log-regression method, the DIC preferred the  
467 model with no random effects. In addition, for the log-GMR subsample, the DIC preferred the

468 normal error structure to lognormal, and equal residual variances to SE-weighted residual  
469 variances. For the complete dataset of log-GMR data, the DIC preferred lognormal error to  
470 normal error, for the subsample, normal was preferred. Considering that the subsampled data is  
471 more balanced across ages, and that the log-GMR is the best back-calculation method, the best  
472 dataset is log-GMR subsample. For this dataset, the DIC prefers the model with constant residual  
473 error, normal residuals, and individual variation in  $L_\infty$  only.

474

475 Although the choice of back-calculation method (log-GMR method 2 versus log-regression  
476 method 3) did not influence which parameters had significant individual variation, it did  
477 influence the amount of individual variation between fish in  $L_\infty$  (Figure 6). Though the models  
478 with individual variation in  $L_\infty$  were generally preferred for all back-calculation models, there  
479 was a greater variation in  $L_\infty$  for the model fitted to log-GMR lengths than to the model fitted to  
480 lengths inferred by log-regression. Individual fish had  $L_\infty$  values that varied from 108 to 135 cm  
481 in the log-GMR model, but only from 116 to 134 in the regression model (Figure 6). The GMR  
482 model (method 1, not shown) was similar to the log-GMR.

483

484 The back-calculation methods influenced the values of the mean for  $L_\infty$  and  $K$ , but not as much as  
485 the sample size and distribution of fish ages in the sample (Figure 7, Table 5). Datasets  
486 dominated by younger fish tended to estimate larger values of  $L_\infty$  and smaller values of  $K$ , but  
487 this effect was less pronounced when random effects were included in the model. When only  
488 measured lengths were used, using the complete dataset, which was dominated by young fish  
489 gave values of  $L_\infty$  and  $K$  similar to those calculated using only young fish (left 3 points in Figure  
490 7). Similarly, when back-calculated lengths were fitted with no random effects, the model  
491 estimated larger values of  $L_\infty$  for the complete dataset than for the subsample (right two points in  
492 Figure 7). The model with a random effect in  $L_\infty$  was less sensitive to sample sizes, with similar  
493 estimates of the mean of  $L_\infty$  for the complete dataset and the subsample (middle points in Figure  
494 7).

495

496 The main difference between the models with and without random effects was the allocation of  
497 variance (Table 5). The random effects model estimated a smaller residual variance  $\sigma_\epsilon$  than the  
498 fixed effects model, because some of the variability in length at age was interpreted as variation  
499 in growth between individuals. The random effects model also estimated a slightly lower  
500 correlation between the mean values of  $L_\infty$  and  $K$ . The model with random effects in  $L_\infty$  implies  
501 that most of the variation in length at age is individual variation (Figure 8). The mean growth  
502 curve is quite similar with or without random effects (Figure 8).

503

504

## 505 Discussion

506

507 We were unable to find any annual variability between cohorts or years in the growth increments,  
508 possibly because we only had two years of captures in the data set. With a longer time series, it  
509 might be possible to evaluate whether some years had larger growth increments than others  
510 within the random effects modeling framework (Shelton and Mangel, 2012).

511

512 The high correlation found between length and spine radius, gave support to the back-calculation  
513 methods applied to derive information about growth for each individual albacore (Ricker, 1992).  
514 The application of GMR methods allowed calculation of a  $y$ -intercept value to be used along  
515 with a proportional method to back-calculate lengths; thus, results were biologically plausible  
516 (Folkvord and Mosegaard, 2002; Ricker, 1992). In this context, the back-calculation proportional  
517 method followed in our approach accommodated previous knowledge on statistical efficiency of  
518 proportional model application (Guteuter, 1987 in Quinn and Deriso, 1999) also applied in other  
519 tuna species (Cheng *et al.*, 2012; Duarte-Neto *et al.*, 2012) and billfishes (Kopf, *et al.*, 2011).

520

521 The deviance information criterion (DIC) preferred the models with individual variation in  $L_\infty$  but  
522 not  $K$  for both the standard log-GMR back-calculation method, and when a simple regression was  
523 used to back calculate lengths. Accordingly, the result that variation exists in  $L_\infty$  but not  $K$  seems  
524 not to depend on the assumption of growth from a common intercept in the back-calculation  
525 model. Thus, we can probably conclude that the result that there is more variation in  $L_\infty$  than  $K$  is  
526 not an artifact of the functional form of GMR back-calculation, as suggested by Francis (1995), at  
527 least for North Atlantic albacore.

528

529 Similar results about individual variation in  $L_\infty$  but not  $K$  were found from analyses on length  
530 increment derived from the release-recapture information available from tagging experiments (  
531 models 3, 4 and 7 and Tagging (equation3) in Table 6). In contrast, another albacore growth  
532 study based on a model that integrated spines and tagging data did not find variability in  $L_\infty$  (last  
533 model in Table 6, Santiago and Arrizabalaga, 2005). None of the analyses, neither those using  
534 tagging data (Table 6) nor our study (Table 5), found individual variation on the growth rate  
535 parameter ( $K$ ). Thus individual variation on  $L_\infty$  only seems to be the most plausible model for  
536 North Atlantic albacore. On the other hand, a simulation study by Eveson *et al.* (2007)  
537 concluded that when variability exists in both growth parameters it is rare that both sources of  
538 variability can be detected; therefore, they recommended using models that include individual  
539 variation in both parameters even if only one was found to vary significantly.

540

541 The means of  $L_\infty$  and  $K$  are consistent with previous studies based on spine readings, or the spine  
542 and tagging data integrated models (Table 6). However, estimates derived from tagging data  
543 were affected by low reporting rates of fish at longer time at liberty and a paucity of return data  
544 for larger fish from commercial fleets, consequently smaller asymptotic  $L_\infty$  were estimated (Table  
545 6, Ortiz de Zárate and Restrepo, 2001; Santiago and Arrizabalaga, 2005). Our estimates, a mean  
546 asymptotic  $L_\infty$  of 120 cm and growth rate ( $K$ ) of 0.21, are nearly identical to the values ( $L_\infty$ =122  
547 cm,  $K$ = 0.209) found by Santiago and Arrizabalaga (2005) based on both spines and tagging data,  
548 and used in the current assessment (ICCAT, 2013b). The introduction of individual variation into  
549 the growth model, which is biologically realistic, does not lead to a substantial change in  
550 expected distribution of lengths at age for this species, given the similar length range covered in  
551 both studies, compare Santiago and Arrizabalaga (2005, their Table 2) to our study (Figure 2).

552

553 Using either all the data or a more balanced subsample gives somewhat different estimates of the  
554 mean  $L_\infty$  and  $K$  parameters (Figure 7). Datasets dominated by younger fish tended to estimate  
555 higher values of  $L_\infty$  and lower values of  $K$ . The mean values of  $L_\infty$  were slightly higher when only

556 measured lengths were used than when the back-calculated lengths were analyzed (Figure 7).  
557 Few large fish were included in the dataset (>90 cm), which may be the reason that small changes  
558 in the modeling assumptions gave different  $L_{\infty}$  results. A dataset that is more informative about  
559  $L_{\infty}$  might be more robust to the choice of estimation methodology. The length range of albacore  
560 samples used in our study represents the selectivity of surface fleets that target albacore in North  
561 Atlantic stock and represent nearly 80% of total catch (ICCAT,2013b; ICCAT, 2014).  
562 Nevertheless, availability of a larger sample of the adult albacore fraction of the population  
563 would improve precision on older albacore aging.

564

565 Our study corroborates the hypothesis of negatively correlated asymptotic mean length ( $L_{\infty}$ ) and  
566 growth rate ( $K$ ) for north Atlantic albacore, as has been found in other species (Helser and Lai,  
567 2004; Pilling et al., 2002). The correlation between  $L_{\infty}$  and  $K$  obtained from the random effects  
568 model (-0.85) is very close to the negative correlation of -0.8 assumed in simulation studies  
569 (Hampton and Majkowski, 1987).

570

571 There are some caveats involved in the use of spines rather than repeated measurements of length  
572 to estimate individual variability in estimate individual variation in growth. The method assumes  
573 that there is a high correlation between spine length and fish length, that the functional  
574 relationship between fish length and spine length is known, and that the relationship does not  
575 change over time or between individuals (Schirripa 2002). We found a clear linear relationship  
576 between log(spine diameter) and log(fork length), which supports this approach (Figure 4).  
577 It is worth noting that estimates of the mean growth parameters based on spine readings at  
578 capture (Measured only, Table 5), yielded similar growth parameters to those calculated with  
579 back-calculated lengths (Table 5, best model, and fixed effects). This could be interpreted as a  
580 verification that the backcalculation is not introducing bias.

581

582 Because of size-selectivity in the fisheries, lengths of fish captured at age one may be skewed  
583 larger than the lengths at age 1 back-calculated from fish caught at older ages. In general, mean  
584 length-at-age 1 estimates from observed length varies across studies (Table 2, Bard, 1981,  
585 Santiago and Arrizabalaga, 2005). In our study, using Method 2 to reconstruct the individual  
586 trajectory by back-calculation estimated the smallest mean length-at-age 1. Size-selectivity may  
587 explain some of the differences between studies, and it is not clear which methods generate the  
588 least biased distribution of lengths at age 1.

589

590

591 Our study advances understanding of growth of the north Atlantic albacore population by  
592 including random effects in the von Bertalanffy growth parameters to model individual variation  
593 on growth. The Bayesian hierarchical modeling approach performed well when incorporating  
594 individual trajectories to model growth of north Atlantic albacore and the fitted model explained  
595 the current growth of the North Atlantic population of albacore. This approach allows testing  
596 hypotheses about the back-calculation method and about the impact of size of the sample and  
597 length coverage for the albacore von Bertalanffy growth model of North Atlantic albacore.  
598 Further research on the uncertainty on age of young albacore (i.e. age one) and the differential  
599 growth rate for sexually mature males and females can be addressed in future analyses.

600 Moreover, the time effect of growth needs to be tested with longer time series to evaluate whether

601 there is year-to-year variability in growth. Future simulations studies to evaluate modeling  
602 growth would contribute to explore uncertainties about the growth of this stock.

603

604

605

606

607

608

609

### 610 **Acknowledgements**

611

612 We would like to thank R.I.C.C. Francis and A. Punt for helpful comments on an earlier draft  
613 data analyses. We also wish to thank P. Quelle, M. Ruiz and O. Gutierrez for the processing of  
614 spine samples. Finally, we thank one anonymous manuscript reviewer and Paul A. Breen, for  
615 their insightful comments that improved the manuscript. This paper was a result of the research  
616 project ATLANTAS3 funded by IEO and partial funded by European Union under the National  
617 Data Collection 2011-2013 Framework Program. E. Babcock's work was supported by the  
618 University of Miami, and by NOAA via CIMAS.

619

### 620 **Author contribution**

621

622 V. Ortiz de Zárate. Design of sampling scheme, aging and back-calculation methods. E. A.  
623 Babcock. Design of growth modeling and analysis conducted in JAGS using the R statistical  
624 software. Both authors wrote manuscript sections and contributed to discussion.

625

626

627

628

629

630

631

632

633

634

635

636

637

638

639

640

641

642

643

644

645

646 **References**

- 647 Bagenal, T. 1978. Methods for assessment of fish production in fresh waters. IBP (International  
648 Biological Programme) Handbook 3, 3rd ed., 365 p. Blackwell Sci. Publ., Oxford.
- 649 Bard, F.X., Compeán–Jimenez, G. 1980. Consequences pour l'évaluation du taux d'exploitation  
650 du germon (*Thunnusalalunga*) nord atlantique d'une courbe de croissance déduite de la lecture  
651 des sections de rayons épineux. ICCAT Col. Vol. Sci. Pap. 9 (2): 365-375  
652
- 653 Bard, F.X. 1981. Le thon germon (*Thunnus alalunga*) de l'Océan Atlantique. Ph.D. Thesis  
654 presented at the University of Paris, 333 p.  
655
- 656 Beamish, R.J., McFarlane, G.A. 1983. The forgotten requirement for age validation in fisheries  
657 biology. Transactions of the American Society 112: 735-743.  
658
- 659 Beverton, R.J. H, Holt, S.J. 1957. On Dynamics of Exploited Fish Populations. Chapman &  
660 Hall. London. Facsimile reprint, 1993.  
661
- 662 Bigelow, K.A., Jones, J.T., Sierra, M.M. 1993. Age variability within length-frequency mode of  
663 the North Pacific albacore fishery as determined by otolith analysis. 13<sup>th</sup> North Pacific Albcore  
664 Workshop, NPALB13/20.  
665
- 666 Bigelow, K.A., Nishimoto, R.N., Laurs, R.M., Wetherall, J.A. 1995. Bias in otolith age estimates  
667 of North Pacific albacore due to microscopy limitations. 14<sup>th</sup> North Pacific Albcore Workshop,  
668 NPALB14/11.  
669
- 670 Bowker, A. H. 1948. A test for symmetry in contingency tables. Journal of the American  
671 Statistical Association, 43: 572-574.  
672
- 673 Campana, S. E. 1990. How reliable are growth back-calculation based on  
674 otolith?. Can.J.Fish.Aquat.Sci, 47: 2219-2227.  
675
- 676 Campana, S. E. 2001. Accuracy, precision and quality control in age determination, including a  
677 review of the use and abuse of age validation methods. Journal of Fish Biology, 59:197-242.  
678
- 679 Campana, S. E., Annand, M. C., McMillan, J. I. 1995. Graphical and statistical methods for  
680 determining the consistency of age determinations. Transactions of the American Fisheries  
681 Society 124:131–138.  
682
- 683 Cheng, Z., Fengying, L., Hao, T., Liuxiong, X., Siquan, T. 2012. Age and growth of Albacore Tuna  
684 (*Thunnus alalunga*) in the southern and central Indian Ocean based on Chinese observer data. In  
685 IOTC–WPTmT04 2012. Report of the Fourth Session of the IOTC Working Party on Temperate  
686 Tunas. Shanghai, China, 20–22 August 2012. IOTC–2012–WPTmT04–R[E]: 43 pp.  
687 <http://www.iotc.org/documents/report-fourth-session-iotc-working-party-temperate-tunas>



688  
689 Duarte-Neto, P., Higa, F.M, Lessa, R.P. 2012. Age and growth estimation of bigeye tuna,  
690 *Thunnusobesus*(Teleostei: Scombridae) in the southwestern Atlantic. Neotropical Ichthyology,  
691 10(1): 149-158, 2012.  
692  
693 Eltink, A.T.G.W. 2000. Age reading comparisons. (MS Excel workbook version 1.0 October  
694 2000).Internet: <http://www.efan.no>  
695  
696 Evans, G. T., Hoenig, J. M. 1998. Testing and viewing symmetry in contingency tables, with  
697 application to readers of fish ages. Biometrics, 54: 620-629.  
698  
699 Eveson, P.G., Polacheck, T., Laslett, G.M. 2007. Consequences of assuming an incorrect error  
700 structure in von Bertalanffy growth models: a simulation study. Can.J.Fish. Aquat. Sci.64: 602-  
701 617.doi:10.1139/F07-036.  
702  
703 Folkvord, A., Mosegaard, H. 2002. Growth and growth analysis, *in*: Panfili, J., Pontual,  
704 H., Troadec, H., Wriqth, P.J. IFREMER-IRD coeditors. Manual of Fish Sclerochronology. Brest,  
705 France, pp. 146- 166.  
706  
707 Francis, R. I. C. C. 1990. Back-calculation of fish length : a critical review. J. Fish.Biol., 83-902.  
708  
709 Francis, R. I. C. C. 1995. The analysis of otolith data - a mathematician's perspective (What,  
710 precisely, is your model?). *in* D. H. Secor, J. M. Dean, and S. E. Campana, editors. Recent  
711 developments in fish otolith research. University of South Carolina Press, Columbia, SC, pp. 81-  
712 95  
713  
714 Fraser, C. M. 1916. Growth of the spring salmon. Transactions of the Pacific. Fisheries Society  
715 1916:29-39.  
716  
717 Gelman, A., Hill, J. 2007. Data analysis using regression and multilevel/hierarchical models.  
718 Cambridge University Press.  
719  
720 Gonzalez-Garcés, A., Fariña-Perez, C. 1983. Determining age of young albacore, *Thunnus*  
721 *alalunga*, using dorsal spines. NOAA, Technical Report NMFS, 8.  
722  
723 Gutreuter, S. 1987. Consideration for estimation and interpretation of annual growth rates. *in*  
724 R.C. Summerfelt and G.E. Hall, eds. The age and Growth of Fish, Iowa State University Press,  
725 Ames, pp. 115-126.  
726  
727 Hampton, J. 1991. Estimation of Southern bluefin tuna *Thunnus maccoyii* growth parameters  
728 from tagging data, using von Bertalanffy models incorporating individual variation. Fish. Bull.  
729 U.S. 89: 577-590.  
730

731 Hampton, J ., Majkowski, J. 1987. An examination of the accuracy of the ELEFAN computer  
732 programs for length-based stock assessment. *in* Pauly, D. and G.P.Morgan (eds.). The theory and  
733 application of length-based methods of stock assessment. ICLARM. Conf.Ser.Manila.203-216 p.  
734

735 Helser, T. E., Lai, H.L. 2004. A Bayesian hierarchical meta-analysis of fish growth: with an  
736 example for North American largemouth bass, *Micropterus salmoides*. *Ecological Modelling*  
737 **178**:399-416.  
738

739 ICCAT,2013a. Report of the 2013 ICCAT North and South Atlantic albacore data preparatory  
740 meeting. *Collect. Vol. Sci. Pap. ICCAT*, 70 (3): 717-829.  
741 [https://www.iccat.int/Documents/CVSP/CV070\\_2014/n\\_3/CV070030717.pdf](https://www.iccat.int/Documents/CVSP/CV070_2014/n_3/CV070030717.pdf)  
742

743 ICCAT,2013b. Report of the 2013 ICCAT North and South Atlantic albacore  
744 assessmentmeeting.*Collect. Vol. Sci. Pap. ICCAT*, 70(3): 830-995  
745 [https://www.iccat.int/Documents/CVSP/CV070\\_2014/n\\_3/CV070030830.pdf](https://www.iccat.int/Documents/CVSP/CV070_2014/n_3/CV070030830.pdf)  
746

747 ICCAT, 2006-2013, ICCAT Manual (Chapter 2. Albacore). International Commission for the  
748 Conservation of Atlantic Tuna. In: ICCAT Publications [on-line]. Updated 2013. [Cited 01/27/].  
749 <http://www.iccat.int/en/ICCATManual.htm> , ISBN (Electronic Edition): 978-92-990055-0-7  
750

751 ICCAT,2014. Albacore Executive Summary Report of the Standing Committee on research and  
752 statistics (SCRS) ICCAT, Madrid, Spain, September 29 to October  
753 2.[https://www.iccat.int/Documents/Meetings/Docs/2014-SCRS-REP\\_ENG.pdf](https://www.iccat.int/Documents/Meetings/Docs/2014-SCRS-REP_ENG.pdf)  
754

755 Kimura, D.K. and Chikuni, S. 1987. Mixtures of empirical distributions: an iterative application  
756 of the age-length key. *Biometrics* 43: 23-35.  
757

758 Kirwood, G.P., Sommers, I.F. 1984. Growth of two species of tiger prawn, *Penaeus esculentus*  
759 *and P. semisulcatus*, in the Western Gulf of Carpentaria. *Aust. J.,Mar.Freshw.Res.*, 35, 703-12.  
760

761 Kopf, R.K, Davie, P.S., Bromhead, D., Peperell, J.G. 2011. Age and growth of striped marlin  
762 (*Kajia audax*) in the Southwest Pacific Ocean. *ICES Journal of Marine Science*, 68 (9), 1884-  
763 1895.doi:10.1093/icesjms/fsr110.  
764

765 Lee, R. 1912. An investigation into the methods of growth determination in fishes by means of  
766 scales. *Publs Circonst.Cons. Per. Int. Explo. Mer*, 63: 3-35.  
767

768 Lee, R. 1920. A review of the methods of age and growth determination in fishes by means of  
769 scales. *Fishery Investigations Series II Marine Fisheries Great Britain Ministry of Agriculture*  
770 *Fisheries and Food* 4(2).  
771

772 Lu, C-P., Ortiz de Zárate, V., Yeh, S-Y. 2007. Morphology of rings on otolith and spine  
773 characters from North Atlantic albacore of 40-44 cm fork length. *Col. Vol. Sci. Pap. ICCAT*,  
774 60(2): 437-442.

775  
776 Lunn, D., Jackson, C., Best, N., Thomas, A., Spiegelhalter, D. 2013. The BUGS Book: A  
777 Practical Introduction to Bayesian Analysis. CRC Press.  
778  
779 Monastyrsky, G.N. 1930. Methods of determining the growth in length of fish by their scales.  
780 Trudy Instituta Rybnogo Khozyaistva 5, 3-44 (in Russian).  
781  
782 McBride, R.S. 2015. Diagnosis of paired age agreement: a simulation of accuracy  
783 and precision effects. ICES Journal of Marine Science; doi: 10.1093/icesjms/fsv047  
784  
785 Ortiz, M. 2014. Review ageing protocol for Atlantic northern albacore (*Thunnus alalunga*). Col.  
786 Vol. Sci. Pap. ICCAT, 70(3): 1314-1325.  
787  
788 Ortiz de Zárate, V., Landa, J, Ruiz, M., Rodríguez-Cabello, C. 2005. Ageing based on spine  
789 sections reading of North Atlantic albacore (*Thunnus alalunga*): precision, accuracy and  
790 agreement. Col. Vol. Sci. Pap. ICCAT, 58(4): 1235-1248.  
791  
792 Ortiz de Zárate, V., Megalofonou, P., De Metrio, G., Rodríguez-Cabello, C. 1996. Preliminary  
793 age validation results from tagged-recaptured fluorochrome label albacore in North East Atlantic.  
794 Col. Vol. Sci. Pap. ICCAT, 43: 331-338.  
795  
795 Ortiz de Zárate, V, Perez, B, and Ruiz, M. 2013. Statistics from the Spanish albacore (*Thunnus*  
796 *alalunga*) surface fishery in the North eastern Atlantic in 2011. Col. Vol. Sci. Pap. ICCAT,  
797 69(5): 2163-2171.  
798  
798 Ortiz de Zárate, V, Perez, B, and Ruiz, M. 2015. Statistics from the Spanish albacore (*Thunnus*  
799 *alalunga*) surface fishery in the North eastern Atlantic, years: 2012-2013. Col. Vol. Sci. Pap.  
800 ICCAT, *in press*.  
801  
801 Ortiz de Zárate, V., Restrepo, V. 2001. Analysis of tagging data from north albacore: von  
802 Bertalanffy growth estimates and catch-at-age. Col. Vol. Sci. Pap. ICCAT, 52(4): 1435-1446.  
803 [https://www.iccat.int/Documents/CVSP/CV052\\_2001/no\\_4/CV052041435.pdf](https://www.iccat.int/Documents/CVSP/CV052_2001/no_4/CV052041435.pdf)  
804  
804 Ortiz de Zárate, V, Valeiras, X., Ruiz, M. 2007. Sampling protocol for skeletal structures of  
805 North Atlantic albacore tuna (*Thunnus alalunga*) and ageing interpretation. Col. Vol. Sci. Pap.  
806 ICCAT, 60(2): 492-506.  
807  
807 Pilling, G. M., Kirkwood, G.P., Walker, S.G. 2002. An improved method for estimating  
808 individual growth variability in fish, and the correlation between von Bertalanffy growth  
809 parameters. Canadian Journal of Fisheries and Aquatic Sciences 59: 424-432. DOI: 10.1139/F02-  
810 022.  
811  
812 Quinn, T., Deriso, R.B. 1999. Quantitative fish dynamics. Oxford University Press, New York.  
813  
814 R Development Core Team. 2012. R: A language and environment for statistical computing. R  
815 Foundation for Statistical Computing, Vienna, Austria.

816  
817 Ricker, W. E. 1992. Back-calculation of fish lengths based on proportionality between scale and  
818 length increments. Canadian Journal of Fisheries and Aquatic Sciences **49**:1018-1026.  
819  
820 Sainsbury, K.J. 1980. Effect of individual variability on the von Bertalanffy growth equation.  
821 Can. J. Fish. Aquat.Sci. 37: 241-247.  
822  
823 Santiago, J.,Arrizabalaga, H. 2005. An integrated growth study for North Atlantic albacore  
824 (*Thunnus alalunga* Bonn. 1788). ICES Journal of Marine Science, 62, 740-  
825 749.doi:10.1016/j.icesjms.2005.01.015  
  
826 Sardenne, F., Dortel, E, Le Croizier,G., Million,J., Lisbonne,M., Leroy,B., Bodin,N., Chassot,  
827 E. 2014. Fisheries Research 163, 44-57. <http://dx.doi.org/10.1016/j.fishres.2014.03.008>  
  
828 Schirripa, M. 2002. An evaluation of back-calculation methodology using simulated otolith data.  
829 Fishery Bulletin 100: 789-799.  
  
830 Shelton, A. O., Mangel, M. 2012. Estimating von Bertalanffy parameters with individual and  
831 environmental variations in growth, Journal of Biological Dynamics **6**:sup2, 3-30  
  
832 Su, Y.-S., Yajima,M. 2014. R2jags: A Package for Running jags from R.  
833  
834 Thorson, J. T., Simpfendorfer, C.A. 2009. Gear selectivity and sample size effects on growth  
835 curve selection in shark age and growth studies. Fisheries Research **98**:75-84.  
836  
837 Von Bertalanffy. 1938. A quantitative theory of organic growth (inquires on growth laws, II).  
838 JSTOR:Hum.Biol.10,181-213.  
839  
840 Zuur, A.F., Ieno,E.E., Elphick, C.S. 2010. A protocol for data exploration to avoid common  
841 statistical problems. Methods in Ecology and Evolution, I, 3-14.doi:10.1111/j.2041-  
842 210X.2009.00001.x  
  
843 Zhang, Z. N.,Lessard,J.,Campbell,A. 2009. Use of Bayesian hierarchical models to estimate  
844 northern abalone, *Haliotis kamtschatkana*, growth parameters from tag-recapture data. Fisheries  
845 Research **95**:289-295.  
  
846  
847  
848  
849  
850  
851  
852  
853  
854  
855  
856

857

858

859 Table 1. Estimated parameters in the full growth model and their priors. For models without  
860 individual variation in a parameter, the values for each individual fish are equal to the population  
861 mean.

862

Parameter	Description	Prior
$L_{\infty,i}$	Individual fish asymptotic length	Normal( $\mu_L, \sigma_L$ )
$K_i$	Individual fish growth rate	Normal( $\mu_K, \sigma_K$ )
$\mu_L$	Population mean $L_{\infty}$	Lognormal(0,1000)
$\sigma_L$	Standard deviation in $L_{\infty}$ between fish	Uniform(0.0001,1000)
$\mu_K$	Population mean growth rate	Lognormal(0,1000)
$\sigma_K$	Standard deviation in $K$ between fish	Uniform(0.0001,10)
$t_0$	Population mean age at $L=0$	Normal(0,1000)
$\sigma_{\varepsilon}$	Standard deviation of the measurement error $\varepsilon$	Uniform(0.0001,100)
$\sigma_{measured}$	Standard deviation of the measurement error $\varepsilon$	Uniform(0.0001,100)
$\sigma_{back}$	Standard deviation multiplier for back calculated lengths	Uniform(0.0001,100)

863

864  
 865  
 866  
 867  
 868  
 869

Table 2. Albacore observed length (cm) and back-calculated length (cm) obtained by the three methods described in the study for the aggregated samples from 2011 and 2012.

Age	Observed Length					BCL Method 1-Fraser-Lee					BCL Method 2-Monastyrsky				BCL Method 3-Regression	
	N	mean	st dev	CV%	SE	N	mean	st dev	CV%	SE	mean	st.dev	CV%	SE	mean	st.de
1	538	53.3	6.49	12.2	0.28	898	52.2	3.7	7.2	0.12	51.8	4.1	7.9	0.14	52.1	3
2	348	64.4	3.97	6.2	0.21	594	63.9	3.9	6.0	0.16	64.2	4.1	6.4	0.17	64.1	3
3	364	74.7	4.42	5.9	0.23	234	74.1	4.4	5.9	0.29	74.8	4.6	6.1	0.30	74.6	3
4	155	83.4	4.53	5.4	0.36	81	84.0	5.2	6.1	0.57	84.9	5.3	6.3	0.59	84.2	3
5	41	90.8	4.09	4.5	0.64	39	93.3	6.3	6.7	1.01	94.1	6.3	6.7	1.00	91.6	4
6	11	99.1	5.45	5.5	1.64	26	100.2	7.8	7.8	1.53	100.7	7.5	7.5	1.48	97.4	3
7	13	106.6	7.87	7.4	2.18	13	100.7	5.3	5.3	1.48	101.1	5.2	5.2	1.45	98.5	3
8	9	102	4.33	4.2	1.44	3	107.8	5.0	4.7	2.90	108.0	5.1	4.7	2.92	103.8	3
9	4	110	4.32	3.9	2.16	1	100.4				101.4				106.3	3
10	1	105				1	103.2				104.0				109.0	3
11	1	108				1	106.9				107.4				112.5	3
Total	1485					1891										

870  
 871  
 872  
 873  
 874  
 875

876 Table 3. Analysis of variance for the model of the effect of numerical age and the factor cohort  
 877 on annual growth increment.

878

	Df	Sum Sq	Mean Sq	F value	Pr(>F)
age	1	3.47	3.47	93.32	<0.0001
cohort	2	0.09	0.04	1.15	0.32
age:cohort	2	0.09	0.05	1.24	0.29
Residuals	1328	49.36	0.04		

879

880

881

882 Table 4. DIC comparison of growth models fitted to lengths back-calculated by the three  
 883 methods. The best growth model for each dataset is the one with  $\Delta_{DIC} = 0$ . All models had  
 884 normally distributed residuals and constant residual variance except where noted.

885

Data	Subsample	Error model	Random effects	$\Delta_{DIC}$
GMR	all data		$L_{\infty}, K$	182.10
			$L_{\infty}$	0.00
			none	135.57
GMR	subsample		$L_{\infty}, K$	112.78
			$L_{\infty}$	0.00
			none	70.35
log-GMR	all data		$L_{\infty}, K$	614.92
			$L_{\infty}$	497.31
			none	893.48
		se weighted	$L_{\infty}$	19.99
		lognormal	$L_{\infty}$	0.00
log-GMR	subsample		$L_{\infty}, K$	129.49
			$L_{\infty}$	0.00
			none	557.78
		se weighted	$L_{\infty}$	47.53
		lognormal	$L_{\infty}$	14.05
log-regression	all data		$L_{\infty}, K$	2611.59
			$L_{\infty}$	2536.50
			none	0.00
log-regression	subsample		$L_{\infty}, K$	5.56
			$L_{\infty}$	0.00
			none	144.66

886

887

888

889

890 Table 5. Medians and 95% credible intervals of estimated parameters from the DIC best model,  
 891 which has individual variation in  $L_\infty$ , with the model with no random effects and the model  
 892 applied to measured fish only shown for comparison. Cor(LK) is the posterior correlation  
 893 between the mean value of  $L_\infty$  and the mean value of  $K$ . Data are subsampled and the log-GMR  
 894 back calculation method was used.  
 895

	Best: $L_\infty$ random	Fixed effects	Measured only
cor(LK)	-0.85	-0.96	-0.96
$\sigma_\varepsilon$	2.38(2.21-2.56)	4.93(4.63-5.26)	4.68(4.26-5.18)
$\sigma_L$	6.6(5.6-7.9)		
$\mu_L$	120.2(117.2-123.3)	123.4(118.7-129.1)	126.1(119.7-134.8)
$\mu_K$	0.21(0.2-0.23)	0.20(0.18-0.23)	0.19(0.16-0.22)
$t_0$	-1.62(-1.76-1.49)	-1.62(-1.89-1.38)	-1.63(-2.01-1.32)

896  
 897  
 898

899 Table 6. Growth parameters estimated by different models applied to tagging data and spine  
 900 readings from previous studies of North Atlantic albacore. The parameters  $\sigma^2_{L_\infty}$  or  $\sigma^2_K$  are the  
 901 estimated standard deviation between individuals, with zero implying no variation found. If no  
 902 value is given, the model did not include individual variation. The parameter  $\sigma^2_\varepsilon$  is the normal  
 903 variance of the residual error and  $\sigma^2_m$  is the release measurement error in the model. Normal  
 904 variance error was estimated for tagging data set ( $\sigma^2_{eT}$ ) and spine data set ( $\sigma^2_{eS}$ ).  
 905

Model	Data	n	Model estimates						
			$L_\infty$ (cm)	$\sigma^2_{L_\infty}$	$K(y^{-1})$	$\sigma^2_K$	$\sigma^2_\varepsilon$	$\sigma^2_m$	$t_0$ (y)
von Bertalanffy model [1]	Spines	352	124.7		0.23				-0.989
Model 3 [2]	Tag data	298	105.6	59.1	0.33		12.4		
Model 4 [2]	Tag data	298	105.6	68.7	0.33		7.7	7.6	
Model 7 [2]	Tag data	298	105.6	68.7	0.33	0	7.7		
Tagging (Equation 3) [3a]	Tag data	309 <sub>a</sub>	110.5	55.04	0.29		12.9		
von Bertalanffy model [3b]	Spines	761 <sub>b</sub>	127.1		0.18		21.7		-1.616
von Bertalanffy model [3a+b]	Spines+Tag	a + b	122.2	0	0.21		21.56 <sub>T</sub>		-1.338
							22.15 <sub>S</sub>		

[1] Bard, 1981, von Bertalanffy model.

[2] Ortiz de Zárate and Restrepo, 2001, using von Bertalanffy models adapted by Hampton (1991).

[3a] Santiago and Arrizabalaga, 2005, using von Bertalanffy models adapted by Hampton (1991).

[3b] Santiago and Arrizabalaga, 2005, spines von Bertalanffy model.

[3a+b] Santiago and Arrizabalaga, 2005, spines + tag joint analysis von Bertalanffy model.

906  
 907



908 **Figure captions**

909

910 Figure 1. Map of the study area in the Northeast Atlantic Ocean. Albacore spine samples  
911 locations in 2011 and 2012.

912 Figure 2. Length frequency distribution of sampled albacore. Years 2011 and 2012 combined.

913 Figure 3. Residuals and QQ-normal plots of the residuals from (a-b) a linear regression of length  
914 against spine diameter, and (c-d) a linear regression of log(length) against log(spine diameter).

915 Figure 4. (a) Measured lengths and mean line for each kind of regression, and lengths predicted  
916 from each spine diameter using (b) GMR, (c) log-GMR and (d) log-linear regression, with  
917 measured lengths shown for comparison.

918 Figure 5. Sample sizes used in growth model fitting, for (a) all measured and back-calculated  
919 lengths, (b) fish subsampled so that sample sizes are more equal, (c) only young fish (1-5 age),  
920 (d) all measured lengths, and (e) measured lengths subsampled so samples sizes are more equal,  
921 and (f) only young measured fish with an equal sample size.

922 Figure 6. Histograms of the median values of  $L_{\infty}$  across individual fish, from the DIC best model  
923 by back-calculation method (a) log-GMR, and (b) log-linear regression. These models were  
924 calculated from a subsample of the data and had individual variation in  $L_{\infty}$  only.

925 Figure 7. Median and 95% credible intervals of the population mean values of (a)  $L_{\infty}$  and (b)  $K$   
926 for models fitted to the log-GMR data, with varying sample sizes and with and without random  
927 effects in  $L_{\infty}$ . The results from models with measured data only are shown for comparison.

928 Figure 8. The best model applied to the subsampled data from the log-GMR back-calculation.  
929 The solid line is the median growth curve, grey lines are individual growth curves, and points are  
930 length data. Growth model parameters fitted (mean  $L_{\infty} = 120.2$ ;  $K=0.21$ ;  $t_0 = -1.62$ ). The growth  
931 curve fitted to the same data using fixed effects, and the curve fitted to a subsample of measured  
932 data only are shown for comparison (black dotted lines).

933

934 Figure A1. Priors and posteriors for the estimated parameters in the model fit to a subsample of  
935 measured data (a-d), a subsample of measured and log-GMR back-calculated data with fixed  
936 effects only (e-h), and the best model for the log-GMR data, with a random effect for  $L_{\infty}$  (i-m).

937

938 **Appendix.**

939

940 All of the models had Gelman-Rubin diagnostic values near one and an effective sample size  
941 greater than 100, which indicates that the MCMC has adequately converged on the posterior  
942 distribution (Lunn *et al.* 2013). Also the Bayesian P value, which is a diagnostic of model  
943 adequacy, was close to 0.50, as expected for good model fit (Table A1). For two representative  
944 models, the priors and posteriors of the estimated parameters are shown in Figure A1. The  
945 priors were all uninformative. The fact that the posteriors are well estimated and relatively  
946 narrow implies that the data were sufficiently informative to estimate these parameters.

947

948 **Table A1.** Diagnostics of model convergence and fit. The effective number of parameters should  
 949 be more than 100 and the GR diagnostic near 1.0 for MCMC convergence. The Bayesian P value  
 950 is a summary of the residuals, which should be near 0.5 for an adequate model fit.

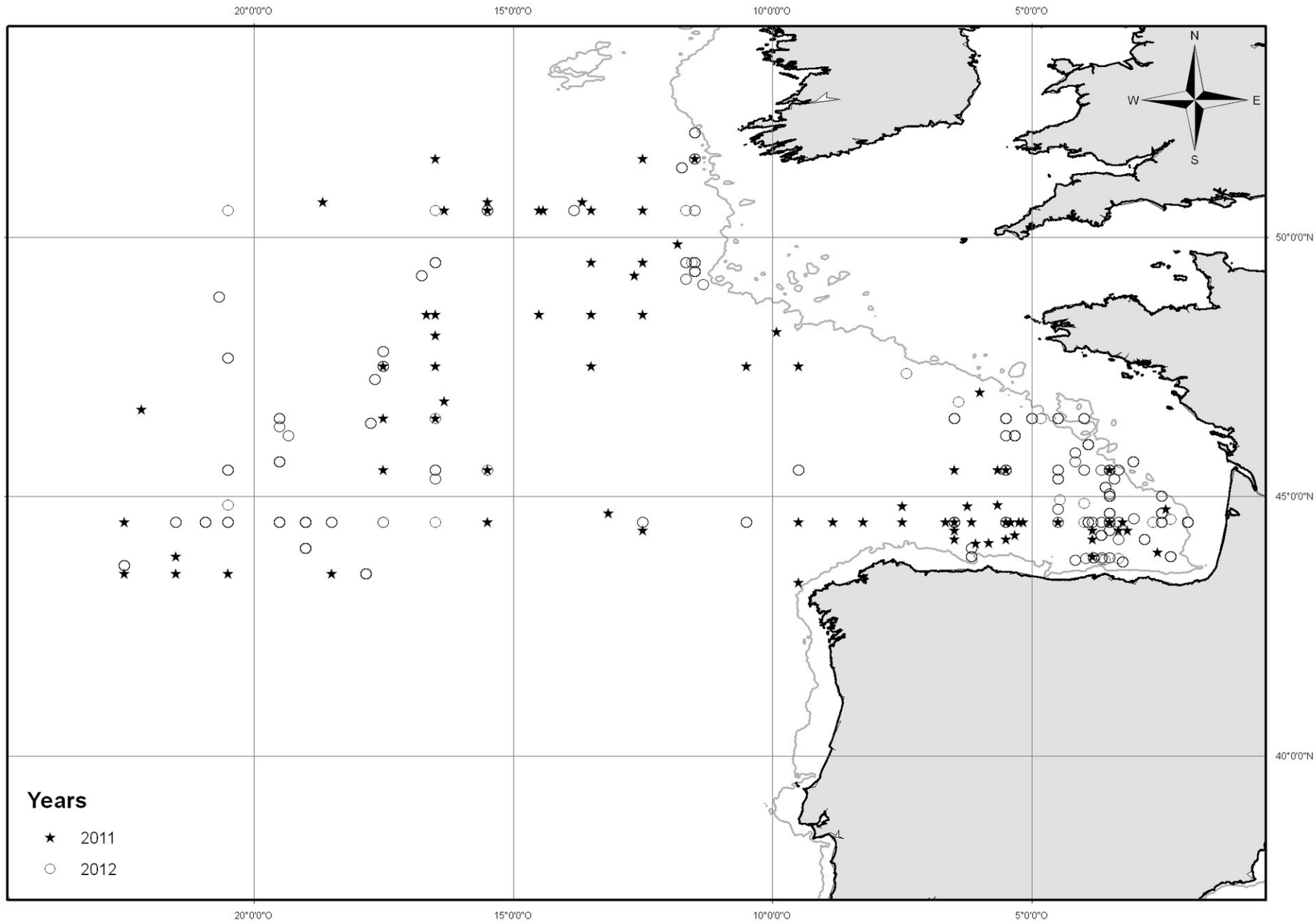
951

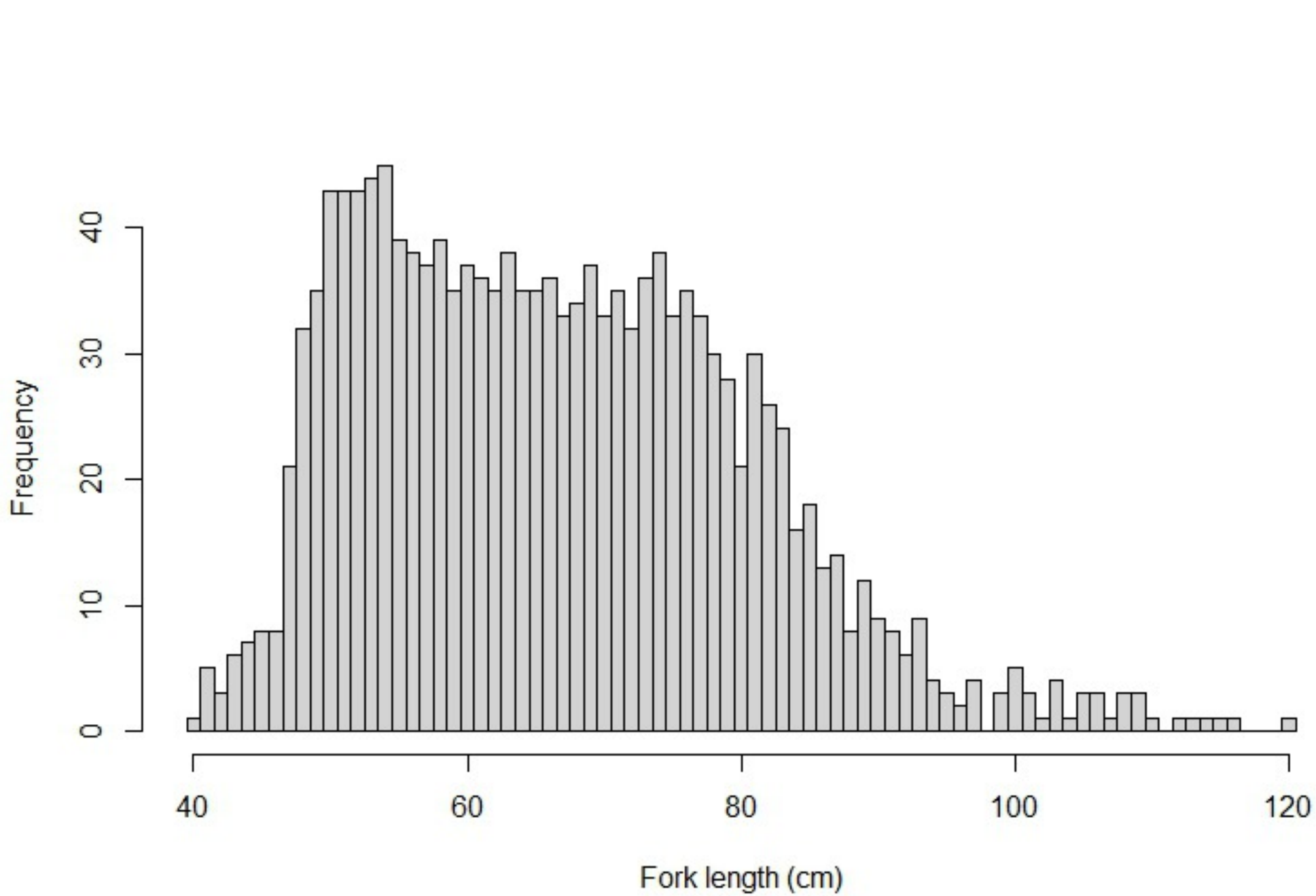
952

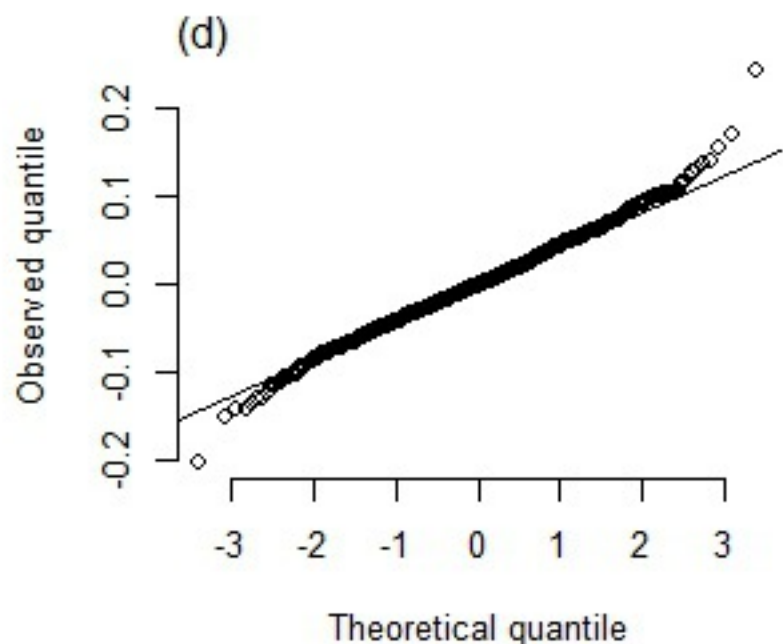
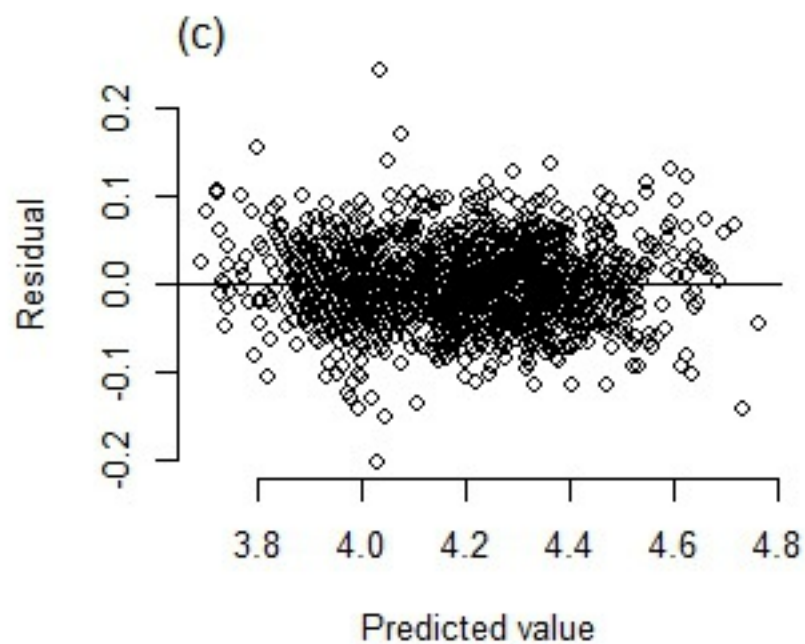
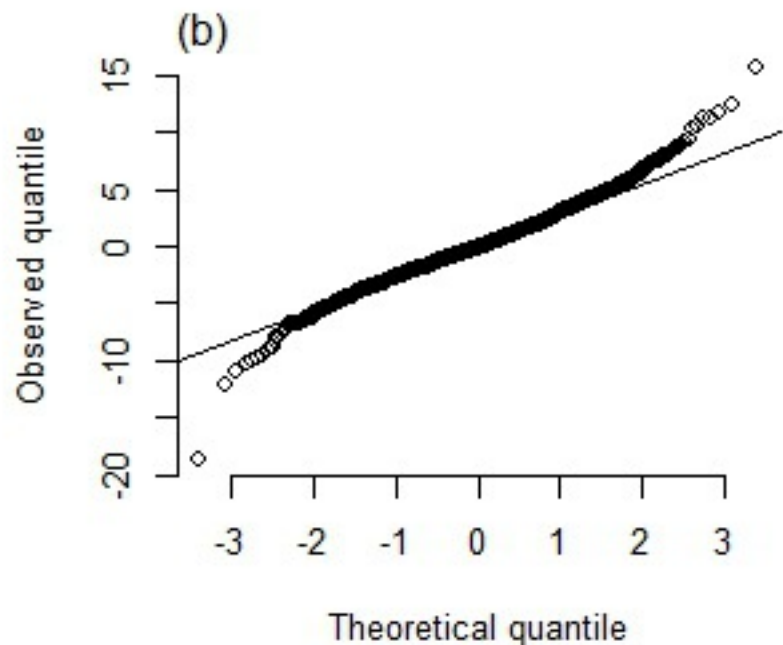
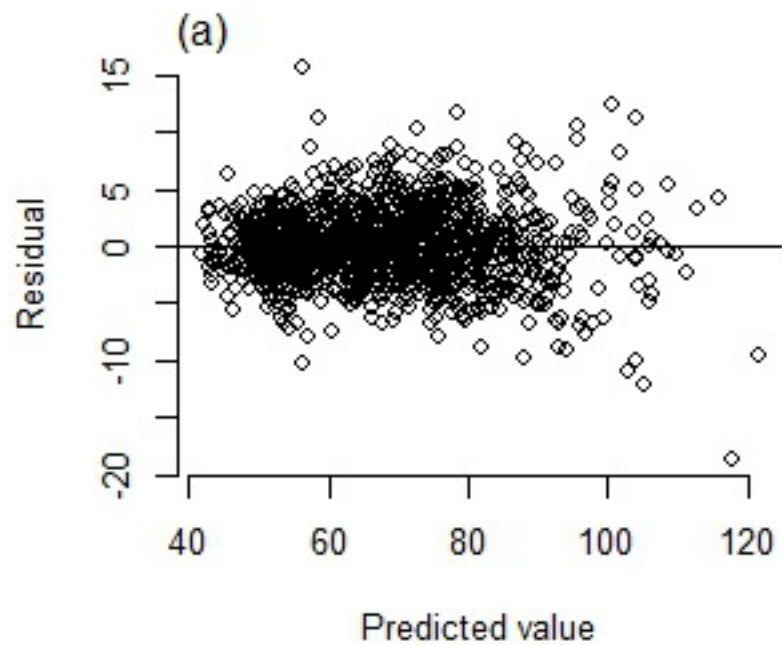
Data	Subsample	Error model	Random effects	Effective n	GRD	P value
GMR	all data		$L_\infty, K$	1200	1.01	0.50
			$L_\infty$	100	1.02	0.50
			none	2800	1.00	0.49
GMR	subsample		$L_\infty, K$	430	1.01	0.50
			$L_\infty$	310	1.01	0.50
			none	480	1.00	0.49
log-GMR	all data		$L_\infty, K$	490	1.01	0.50
			$L_\infty$	100	1.02	0.50
			none	2400	1.00	0.50
		se weighted	$L_\infty$	1200	1.00	0.49
		lognormal	$L_\infty$	110	1.01	0.50
	log-GMR	subsample		$L_\infty, K$	870	1.00
			$L_\infty$	2100	1.00	0.49
			none	1400	1.00	0.49
			se weighted	$L_\infty$	4100	1.00
	lognormal	$L_\infty$	360	1.01	0.48	
log-GMR	young only		$L_\infty$	630	1.00	0.50
log-regression	all data		$L_\infty, K$	560	1.02	0.50
			$L_\infty$	710	1.00	0.50
			none	1300	1.00	0.50
log-regression	subsample		$L_\infty, K$	1000	1.02	0.49
			$L_\infty$	520	1.00	0.49
			none	6900	1.00	0.50
			$L_\infty$	160	1.02	0.49
Captured	all data		none	340	1.01	0.49
Captured	subsample		none	2600	1.00	0.49
Captured	young only		none	1200	1.00	0.49

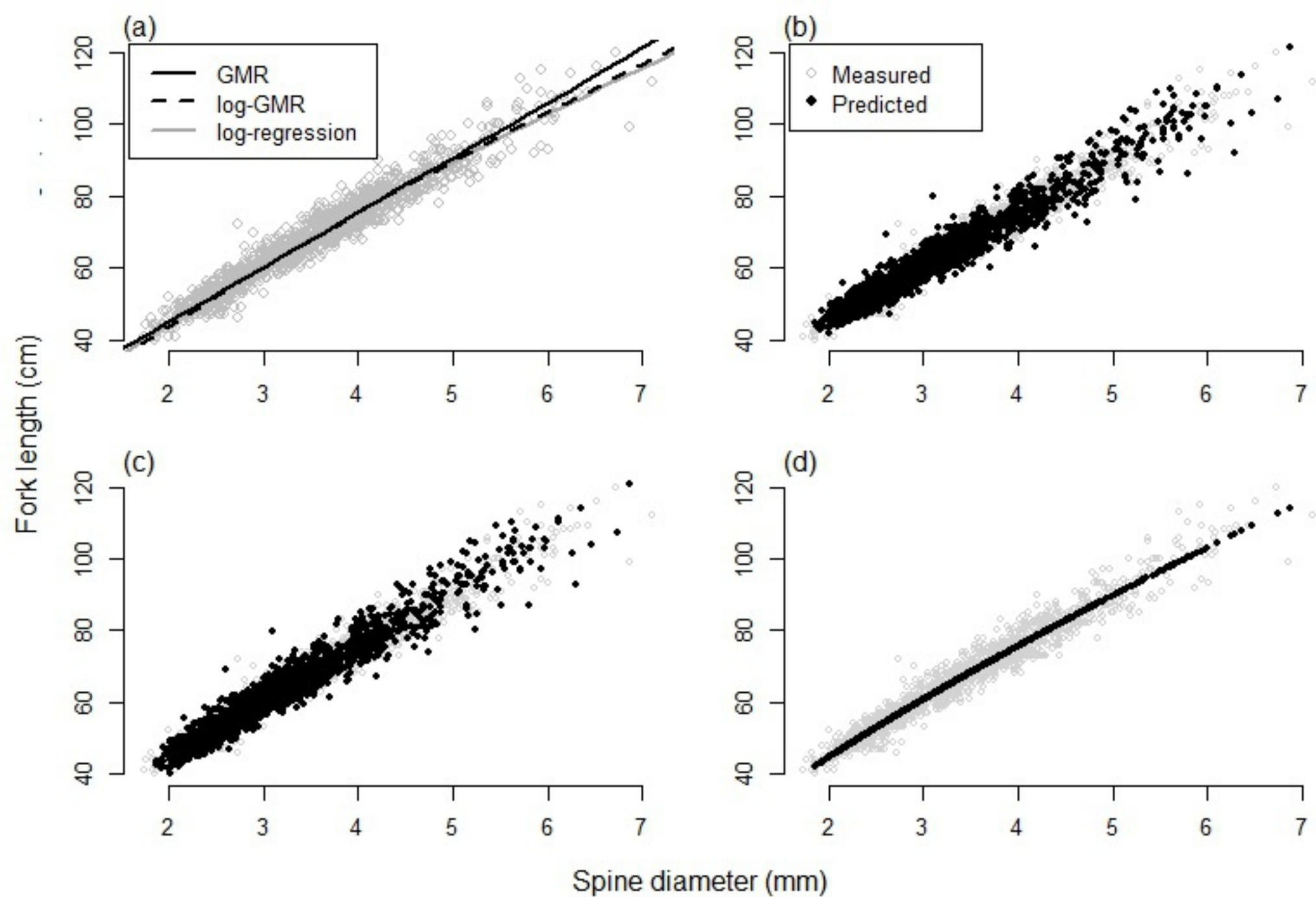
953

954

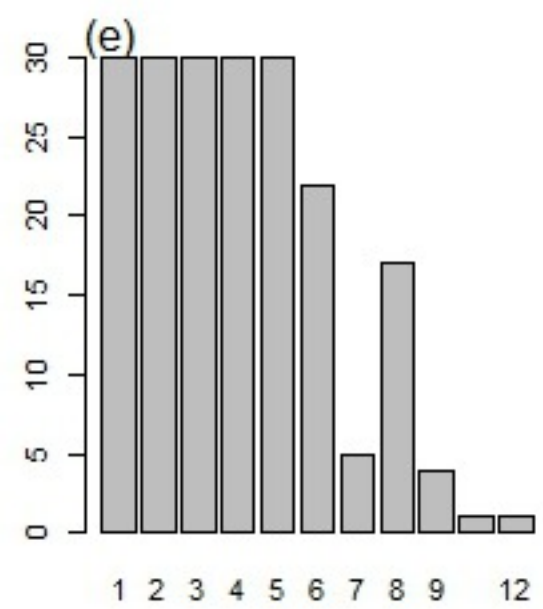
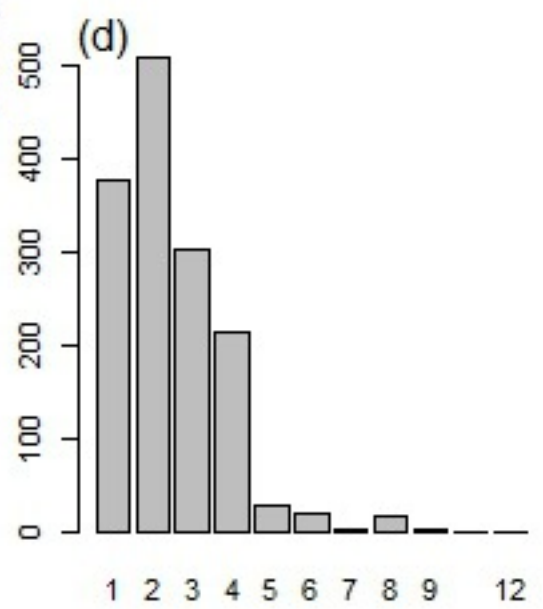
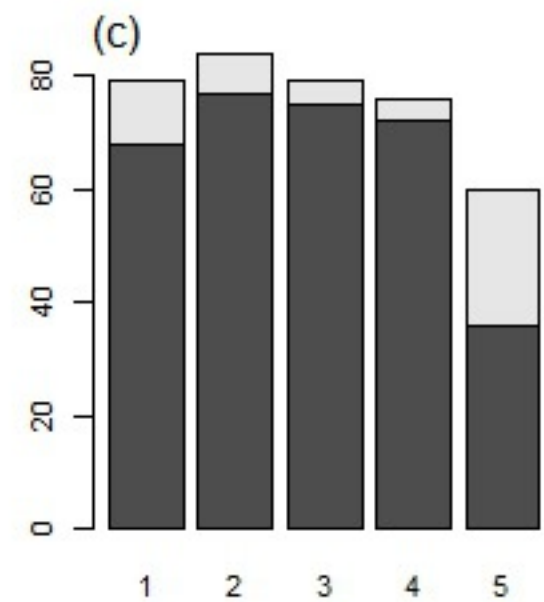
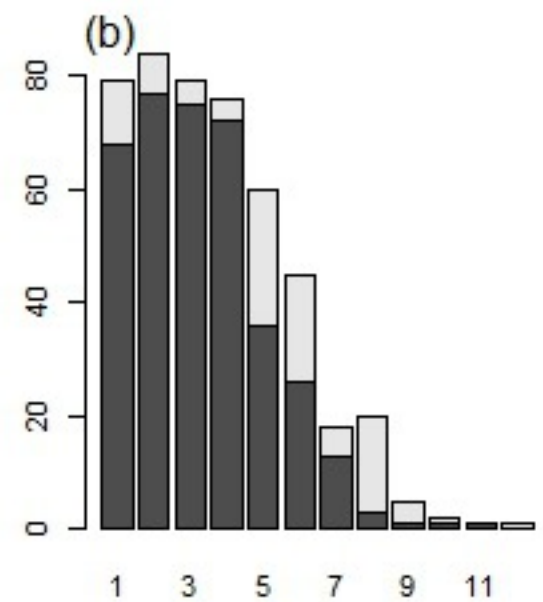
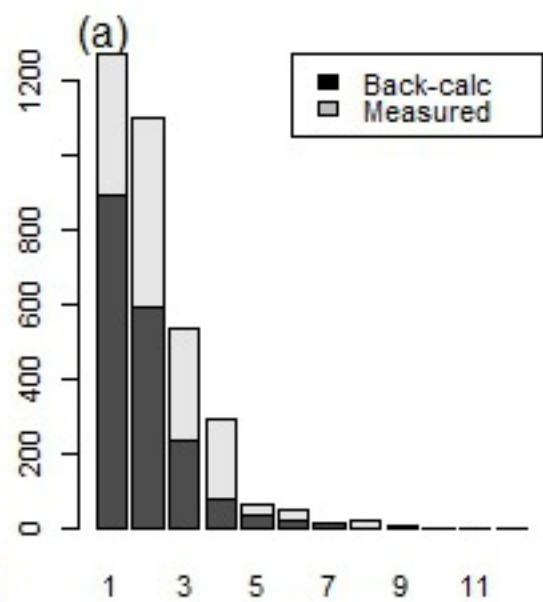








Sample size



Age

